

Simultaneous observation of extensive air showers and deep-underground muons at the Gran Sasso Laboratory

R. Bellotti, F. Cafagna, M. Caliccio, G. De Cataldo, C. De Marzo, O. Erriquez,
C. Favuzzi, N. Giglietto, E. Nappi, and P. Spinelli
Istituto di Fisica dell'Università di Bari, Via Amendola 173, I-70126, Bari, Italy

S. Cecchini, M. Fabbri, G. Giacomelli, G. Mandrioli, P. Matteuzzi, B. Pal,
L. Patrizii, F. Predieri, G. L. Sanzani, P. Serra, and M. Spurio
Dipartimento di Fisica dell'Università di Bologna, Via Irnerio 46, I-40126, Bologna, Italy

S. Ahlen, D. Ficenec, E. Hazen, S. Klein, D. Levin, A. Marin, J. L. Stone,
L. R. Sulak, and W. Worstell
Physics Department, Boston University, 590 Commonwealth Avenue, Boston, Massachusetts 02215

B. Barish, S. Coutu, J. Hong, G. Liu, C. Peck, D. Solie, and J. Steele
California Institute of Technology, Pasadena, California 91125

C. Lane and R. Steinberg
Physics Department, Drexel University, 32nd and Chestnut Street, Philadelphia, Pennsylvania 19104

G. Battistoni, H. Bilokon, C. Bloise, P. Campana, V. Chiarella, C. Forti,
A. Grillo, E. Iarocci, A. Marini, V. Patera, J. Reynoldson, F. Ronga,
L. Satta, M. Spinetti, and V. Valente
Laboratori Nazionali di Frascati, Casella Postale 13, I-00044 Frascati, Roma, Italy

C. Bower, R. Heinz, S. Mufson, and J. Petrakis
Physics Department and Astronomy Department, Indiana University, Swain Hall West, Bloomington, Indiana 47405

P. Monacelli
Dipartimento di Fisica dell'Università di L'Aquila, Piazza dell'Annunziata 1, I-67100, L'Aquila, Italy

P. Bernardini, G. Mancarella, O. Palamara, P. Pistilli, and A. Surdo
Dipartimento di Fisica, Università di Lecce, via per Arnesano 73100, Lecce, Italy

M. Longo, J. Musser, C. Smith, and G. Tarlé
Randall Physics Laboratory, University of Michigan, Ann Arbor, Michigan 48109-1120

M. Ambrosio, G. C. Barbarino, and F. Guarino
Dipartimento di Fisica dell'Università di Napoli, Via Antonio Tari 3, I-80125 Napoli, Italy

A. Baldini, C. Bemporad, V. Flaminio, G. Giannini, M. Grassi, and R. Pazzi
*Istituto di Fisica dell'Università di Pisa, Sezione Istituto Nazionale di Fisica Nucleare,
Via Livornese, 582/A, Pisa, Italy*

G. Auriemma, P. Chrysicopoulou, M. De Vincenzi, M. Iori, E. Lamanna, P. Lipari,
G. Martellotti, S. Petrera, L. Petrillo, G. Rosa, A. Sciubba, and M. Severi
*Istituto Nazionale di Fisica Nucleare, Sezione di Roma, Università di Roma, "La Sapienza,"
Dipartimento di Fisica, Piazzale A. Moro 2, I-00185, Roma, Italy*

P. Green and R. Webb
Texas A&M University, College Station, Texas 77843

V. Bisi, P. Giubellino, A. Marzari Chiesa, M. Masera, M. Monteno, and L. Ramello
Dipartimento di Fisica dell'Università di Torino; Via P. Giuria 1, I-10125, Torino, Italy

(MACRO Collaboration)

M. Aglietta, B. Alessandro, G. Badino, L. Bergamasco, C. Castagnoli,
 A. Castellina, G. Cini, B. D'Ettoire-Piazzoli, W. Fulgione, P. Ghia, P. Galeotti,
 G. Mannocchi, C. Morello, G. Navarra, L. Periale, P. Picchi, L. Riccati,
 O. Saavedra, G. Trincherro, P. Vallania, and S. Vernetto

*Dipartimento di Fisica dell'Università di Torino, Sezione di Torino dell'Istituto Nazionale di Fisica Nucleare,
 Via P. Giuria 1, I-10125, Torino, Italy and Istituto di Cosmo-geofisica del CNR, corso Fiume 4, I-10133, Torino, Italy*

(EAS-TOP Collaboration)

(Received 12 February 1990)

Combined measurements of extensive air showers at the surface and high-energy muons deep underground have been initiated at the Gran Sasso Laboratory. The underground detector is the first supermodule of MACRO (area=140 m², depth=3100 m of water equivalent, $E_{\mu} > 1.3$ TeV) and the surface detector is the EAS-TOP array (altitude 2000 m above sea level, total enclosed area $A \sim 10^5$ m²). We discuss the correlation technique, the comparison between the shower parameters as determined by the two detectors, and some of the characteristics of the reconstructed events.

I. INTRODUCTION

One of the most important problems in high-energy cosmic-ray physics is the study of primary flux at energies above $E_0 = 10^{15} - 10^{16}$ eV where a steepening, or "knee," of the all-particle primary spectrum is observed.¹ In this range of energy the experimental data are still poor and many questions, such as the astrophysical origin of the "knee" or the chemical composition of the spectrum, are still left without a quantitative answer. A precise knowledge of the abundances and spectral indices of the different mass groups of nuclei is of extreme importance in order to have a better understanding of sources of cosmic rays and their propagation and acceleration mechanisms in our Galaxy. In the high-energy region, only indirect measurements of primaries are possible at the present time. Two techniques that can be exploited in this field are (i) the measurement at ground level of secondary electromagnetic cascades [extensive air showers (EAS)] generated by the interaction of a primary particle with the atmospheric nuclei,² by sampling the shower front with large-area surface arrays, and (ii) the measurement of penetrating high-energy muons in underground experiments;³ these muons detected deep underground are the high-energy remnants of the primary interactions.

After the pioneering experiments of Barret *et al.*⁴ about 40 years ago, these two research lines have been pursued mostly by independent experiments, not correlated with each other. The advantage in an event-by-event combined experiment is that it is possible to isolate the very-high-energy region of the primary spectrum and simultaneously measure more physical parameters related to those events. For example, the main uncertainty in the analysis of multimMuon events in underground experiments is the fact that the contribution to a given muon multiplicity comes from primaries whose energies span at least two decades in a differential energy spectrum which is falling as $E_0^{-2.7}$. The composition is therefore difficult to unfold and the sensitivity can be enhanced by correlating the underground multimMuon events with the measurement of the shower size on the surface. This then determines the primary energy for these events to within a fac-

tor of 2 independent of composition. As a consequence it is possible to measure muon multiplicities in fixed-shower-size windows, corresponding to comparable total energies for all nuclear species.

The Gran Sasso Laboratory⁵ (LNGS) offers unique possibilities to accurately perform combined measurements. Previously two experiments have been reported that demonstrate the possibility of making coincidences, but with less extensive detectors.^{6,7} New experiments now in operations at LNGS can provide data on simultaneous observations of EAS and underground muons, with large acceptance and combined reconstruction capability never reached by the past experiments.

In this paper we report the first results obtained by the joint collaboration of the surface EAS-TOP experiment, at 2000 m above sea level, and the underground MACRO experiment, at a depth of 3100 m of water equivalent (m.w.e.). We show the detection features achieved by the two combined experiments, discussing in particular their capability for good reconstruction of cosmic-ray events.

II. THE EXPERIMENTAL APPARATA

Figure 1 shows the location of the surface array and of the underground laboratory with respect to each other. MACRO is located in Hall B of the Gran Sasso underground laboratory (latitude 42° 27' North, longitude 13° 34' East), at an altitude of about 963 m above sea level (a.s.l.). The Eas-TOP array is located above the Gran Sasso underground laboratory, at 27.5° with respect to vertical of MACRO, in correspondence to the minimum thickness of rock, at the altitude of 2005 m a.s.l.

The shower detector in EAS-TOP (Ref. 8) consists of 29 stations separated by 17 m near the center, and 80 m at the edges of the field, each one containing a 10-m² module of scintillator. However in the period corresponding to the data presented here, only 22 stations were operational. The total covered area is about 10⁵ m². Each 10-m² module consists of 16 scintillation counters. Four modules are liquid scintillator, the others NE102A plastics. At present each scintillator is viewed by one photomultiplier tube (PMT) for timing and amplitude

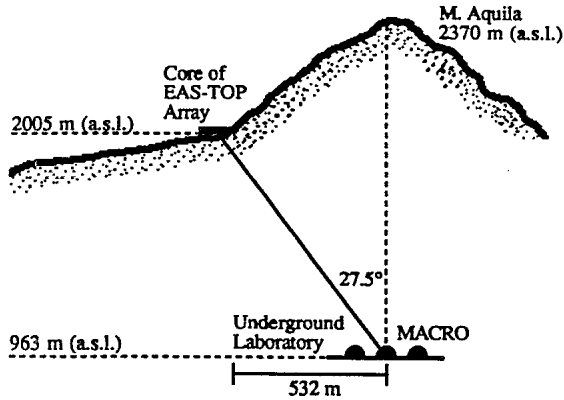


FIG. 1. Locations of the two arrays at the LNGS.

measurements and the gain is equalized to measure a number of particles $n \leq 100$. Typically, at $n = 50$, the error on the determination of the number of particles is about 20%. The threshold of each module is set to an amplitude equivalent to 0.3 minimum-ionizing particles.

For triggering purposes EAS-TOP is organized in seven hexagonal overlapping subarrays of six or seven modules interconnected with each other. The subarrays operate independently. Any coincidence within 500 ns of all the modules within a subarray, triggers the data acquisition of the whole apparatus. In this configuration the measured trigger rate is ~ 5 Hz. Data are taken by means of a microVAX connected through a radiotelephone link to the INFN national network. The absolute timing of the events is provided by a quartz clock (absolute precision $\sim 100 \mu\text{s}$), adjusted by the time standard provided by the Italian national broadcasting company. The EAS-TOP array is able to determine the main shower characteristics with the following resolutions at $E_0 = 10^{15}$ eV: $\sim 1^\circ$ for the direction measurements, a few meters for the core location; $\sim 20\%$ for the shower size N_e ; and 10% for the shower age s [the Nishimura-Kamata-Greisen⁹ formalism is used for lateral distribution function: $\rho(r) \propto N_e(r/r_1)^s - 2(r/r_1 + 1)^{s-4.5}$ with r_1 roughly equal to 100 m at our observation level]. The present trigger scheme gives a calculated efficiency increasing from $\sim 10\%$ at $N_e = 10^4$, corresponding roughly to 100 TeV, to full efficiency at $N_e \sim 10^5$ for showers having the core within the geometrical area defined by the array. The effective detection area depends on the energy, and ranges from 10^4 to over 10^5 m², increasing with energy.

The MACRO detector is a large-area multipurpose experiment.¹⁰ It is designed as a modular array of liquid-scintillation counters, plastic streamer tubes, and track-etch detectors. When complete it will fill a box-shaped volume with 12×78 m² base and 9 m height. The first "supermodule" of MACRO ($12 \times 12 \times 5$ m³) has been operated since the beginning of 1989. It consists of a horizontal sandwich of two scintillation counter layers for timing, 10 streamer tube layers for tracking, and one track-etch multilayer (CR39 and Lexan with an aluminum absorber) to identify highly ionizing particles. Passive absorbers (iron and CaCO_3) are in between the sensitive layers, to identify penetrating particles, setting a

threshold for through-muons pointing at EAS-TOP at 1.2 GeV. Only two sides of the first supermodule are presently closed by one layer of scintillation counters and six layers of streamer tubes.

The streamer tube layers consist of 8-tube PVC chambers, with dimensions 25×3 cm² \times 12 m. The individual cell cross section is 3×3 cm², with a 100- μm anode wire and a graphite cathode. They operate in the limited streamer mode. Two-dimensional localization is performed by 3-cm-wide pick-up strips at an angle of about 30° . The achieved space accuracy is about 1 cm, resulting in an angular accuracy of $\sim 0.2^\circ$ in the two projected views.

The liquid-scintillation counters are 75 cm wide, 26 cm thick, and 12 m long. They are viewed at each end by two PMT's. The trigger energy threshold is ~ 10 MeV, the timing accuracy 1 ns.

Different muon triggers operate independently in MACRO, based on streamer tubes and scintillators, alone or in combination. The measured rate of muons with a selected minimum track length of 180 cm, is ~ 2 per minute. Data are taken through CAMAC managed by microVAX, operating in a VAXELN system, under the control of a VAX 8200. The absolute timing of the events is provided by a rubidium clock (absolute precision $\sim 1 \mu\text{s}$). The clock stability is periodically checked with the radio signal in the external laboratory.

EAS-TOP is seen by MACRO in the angular range 25° – 37° in zenith, and 160° – 200° in azimuth. The rock depth between the two experiments ranges from 3100 to 3500 m.w.e., depending on the angle. The corresponding energy threshold for a muon to be detected underground is $E_\mu = 1.3$ – 1.6 TeV. The time of flight between the two sites, for a relativistic particle, is $\sim 3 \mu\text{s}$.

III. DATA SELECTION

The two experiments have been running simultaneously in the period from 23 March to 29 May 1989, for a total live time of 1107 h.

No physical link at present exists between EAS-TOP and MACRO, so the correlation of data is established off line, on the basis of the absolute timing and the directional capabilities of the detectors. Figure 2 shows the distribution of the time difference between the reconstructed events of MACRO and EAS-TOP, when looking for time coincidence within a 6-ms window, for a subsample of 637 h. No directional cuts are applied at this stage. The peak of correlated events is clearly seen above the background of accidentals. The correlation peak is well fitted by a Gaussian, with a mean value of 3.2 ms (due to a different internal zero setting of the two clocks), and $\sigma \sim 90 \mu\text{s}$. The time resolution is slightly better than expected by the design features of the quartz clock.

The accidental coincidence background can be largely cut by means of directional criteria. Figure 3 shows the same Δt distribution of Fig. 2 when a nonstringent angular cut $\psi \leq 10^\circ$ is applied to the angle in space between the two reconstructed directions. It can be seen that even in this preliminary analysis only a few events are lost with

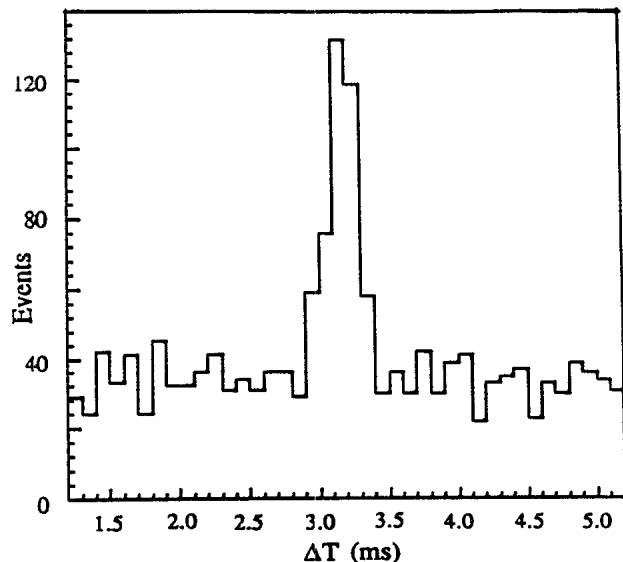


FIG. 2. Time difference distribution of the reconstructed events of EAS-TOP and MACRO in coincidence within 6 ms.

this cut. The area under the correlation peak within $\pm 3\sigma$ in the time corresponds to 8.0 ± 0.7 correlated events per day. The estimated accidental contribution is $\sim 4\%$. In the following we shall maintain the requirement $\Delta t = 3.2 \pm 0.3$ ms to define a coincidence.

With this selection the total number of coincidences found in the whole data sample is 347. The measured coincidence rate is in rough agreement with a preliminary calculation based on the commonly used models of cosmic-ray spectrum and composition, the dependence on energy of the effective area of EAS-TOP, the acceptance cone between the two detectors, and the parametrization of muon propagation in the rock as a function of energy for each primary mass group.¹¹ The coincidence rate has remained constant, within the statistical error, during the entire measurement period, as shown in Fig. 4, where the coincidence rate is shown for different days of the run.

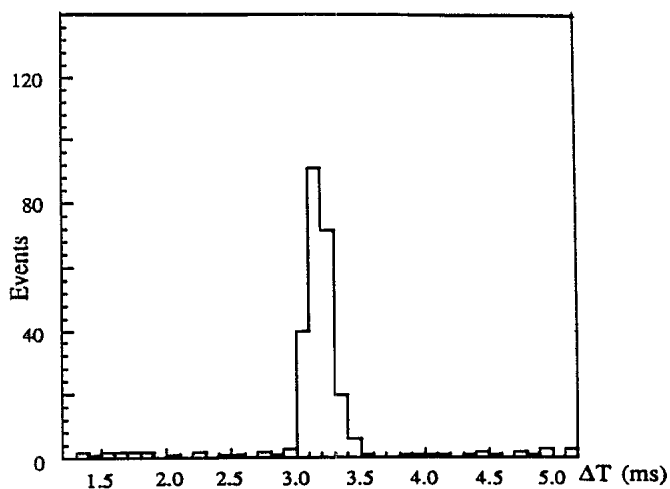


FIG. 3. Same as Fig. 2, when an angular cut $\psi \leq 10^\circ$ is applied to the angle in space between the two reconstructed directions.

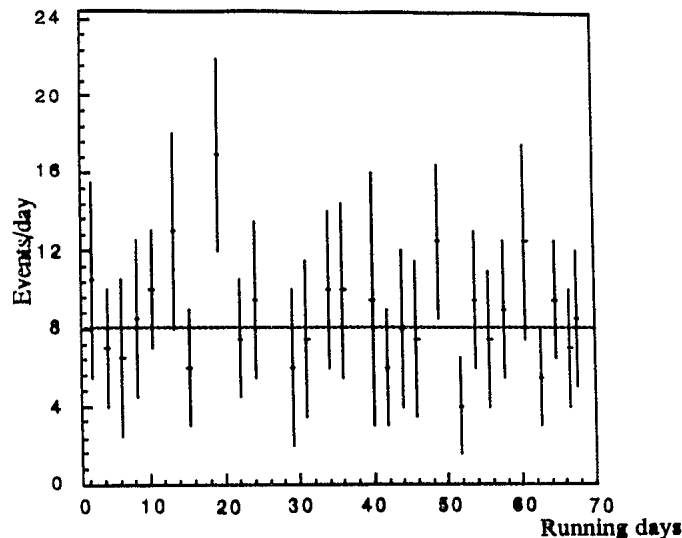


FIG. 4. Rate of correlated events (day^{-1}) as measured in different days of run.

IV. SPATIAL AND ANGULAR RESOLUTION OF THE CORRELATED EVENTS

The reconstruction of the direction of the shower and its core location are obtained independently by the two experiments EAS-TOP uses the different arrival times of the electrons to fit the direction of the showers, and the number of particles in each counter to determine the core location, the shower size, and the lateral distribution of the particles. MACRO uses the tracking of the underground muons to define the arrival direction of the showers; in addition the extrapolation of the tracks of singles muons (or of the center of gravity of multimurons) up to the EAS-TOP plane gives a measurement of the core location.

The achievable accuracies in the event reconstruction depend on physical and instrumental effects. In the case of EAS-TOP the main physical uncertainty is given by the time and density fluctuations of the particles inside the shower disk; this is more relevant far from the shower axis and at the lower energies. The instrumental accuracy is mainly related to the time-to-digital-converter (TDC) system, which must be carefully and frequently calibrated.

In the case of MACRO the tracking system is able to define the arrival direction of a muon with high and stable accuracy, but one has to take into account the multiple scattering of muons in the rock, beyond sparse high- p_t interactions, which give an angular resolution $\sigma_\theta \sim 0.6^\circ$ on the whole. This has been estimated by the distribution of the angle between different tracks in muon bundles. The accuracy in the shower core location by MACRO depends also on the possibility of sampling the muons far from the shower axis. This can introduce a few meters bias at low detected muon multiplicity, but which rapidly vanishes as multiplicity increases. Taking into account all the possible effects, including the back pointing on the surface, the estimated accuracy in the shower-core location at EAS-TOP level for single-muon

events in MACRO is ~ 20 m, decreasing to a few meters at higher muon multiplicities.

In Figs. 5(a)–5(c) we show an example of coincidence event as reconstructed by EAS-TOP and MACRO, respectively; in Fig. 5(a) the measured number of particles is shown for each module; in Fig. 5(b) the lateral distribution function of the shower is fitted to the measured particle densities: from this fit the shower size, age, and core location are derived; in Fig. 5(c) the underground muon event is shown as seen in the two projections of the MACRO supermodule. The muon tracks are fitted with straight lines.

In order to have a first understanding of the reconstruction capabilities of the two combined experiments, as far as the spatial parameters of the showers are concerned, we have restricted our selection to the “internal trigger” events. These are the events in which the largest number of particles is recorded by an EAS-TOP counter not belonging to the edge of the array. In our whole sam-

ple, corresponding to the 1107 h of run, the number of internal trigger events is 93 out of a total of 347.

Figures 6(a)–6(c) show the distribution of the projected angular difference along X (West-East direction), along Y (South-North direction), and of the angle in the space between the reconstructed directions for the two experiments, when a loose cut $\Delta X, \Delta Y \leq 60$ m is applied to the difference of the measured core location coordinates (90 events out of 93). The measured resolutions are $\sigma_{\theta_X} = 1.0^\circ$ and $\sigma_{\theta_Y} = 1.2^\circ$. The average $\Delta\theta_X$ is 0.04 ± 0.10 , and the average $\Delta\theta_Y$ is -0.20 ± 0.12 , showing that no appreciable systematic effects are seen in the angular reconstruction. The corresponding resolution in the angle ψ in space is $\sigma_\psi = 1.5^\circ$; it defines the accuracy in the relative pointing between MACRO and EAS-TOP. In the following we shall consider as coincidences the events passing the 95% cut $\psi \leq 5^\circ$ (87 out of 93).

Figures 7(a) and 7(b) show the distribution of the difference in the shower core location by the two experiments, as projected along two orthogonal axes in a plane perpendicular to the direction EAS-TOP–MACRO. X is again the West-East direction. A resolution of 21 and 15 m is found, respectively, in agreement with the expectations depending on the geometry of the surface apparatus. If a cut is introduced both in the shower size ($N_e \geq 10^5$) and in muon multiplicity ($N_\mu \geq 2$), the above resolutions improve down to 11 and 6 m, respectively.

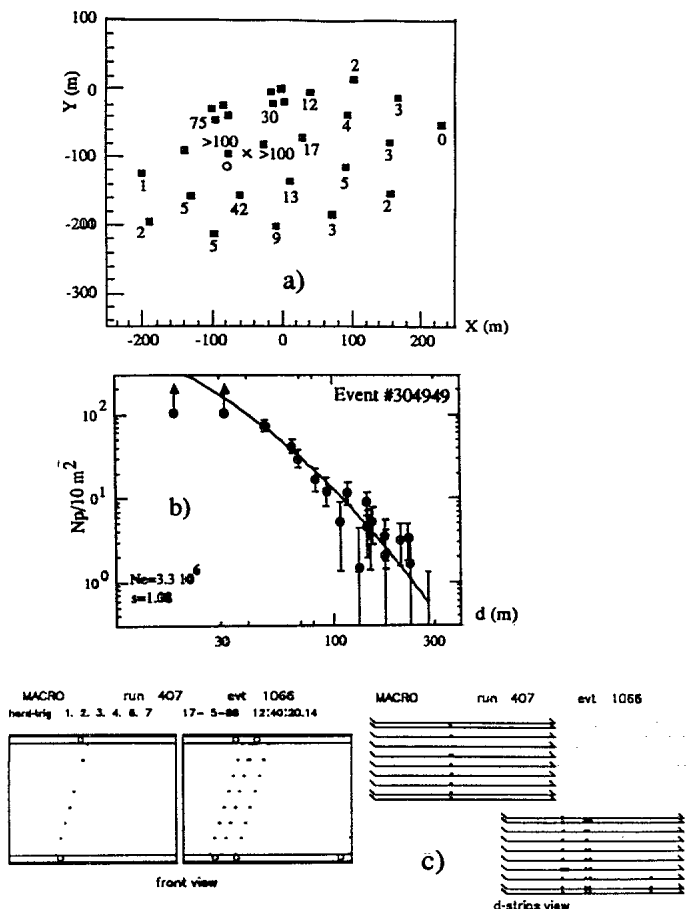


FIG. 5. Example of a coincidence event as seen by the two experiments: (a) number of detected particles in each counter of EAS-TOP; the shower core location as measured by the two experiments are also shown (MACRO, circle; EAS-TOP, cross); (b) reconstructed lateral distribution function, the fitted size and age of the shower are also shown; (c) the two views in the digital tracking of MACRO representing the underground multimMuon event detected in coincidence. The straight-line fits are not reported to allow a better visualization of the hit streamer tubes.

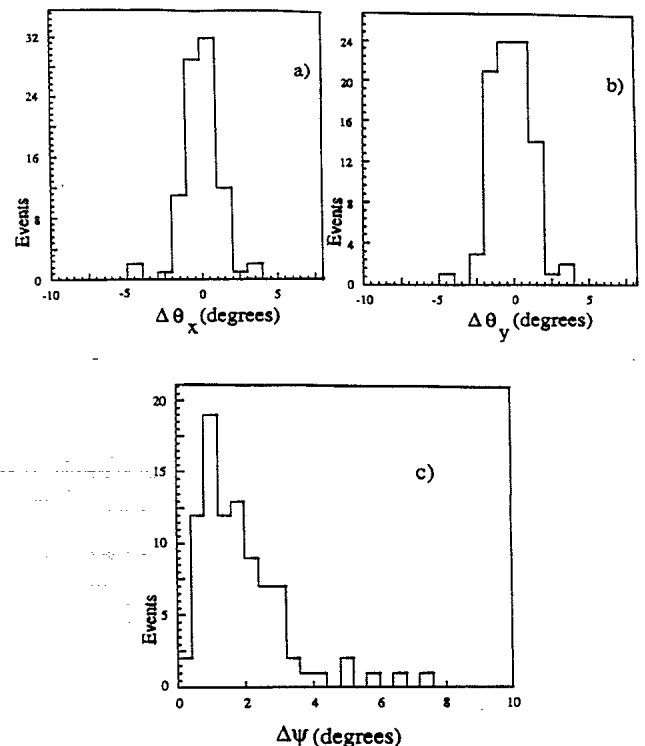


FIG. 6. (a) Angular difference between the directions by the two experiments for the coincident internal trigger events, projected along the West-East direction, and (b) the South-North direction; (c) angle in space between the two reconstructed directions.

V. CORRELATION OF PHYSICAL QUANTITIES

Figure 8 shows the muon multiplicity distribution for the 87 selected internal trigger events. It must be compared to the total multiplicity distribution as measured by MACRO alone. This is reported in the same figure, normalized at $N_\mu = 1$; it refers to a sample of muons corresponding to 1740 h of run, with $\theta \leq 70^\circ$. The different ratio of multiple-to-single muons in the two cases is a direct reflection of the higher primary energy threshold in the coincidence experiment.

Figure 9 shows the measured $\log_{10} N_e$ distribution for the internal trigger sample. The shape of the distribution for $N_e < 10^5$ is affected by the EAS-TOP trigger, and by the requirement of detecting at least one muon in MACRO. The above result shows that this correlation experiment has a good sensitivity in the energy region of the knee of the primary spectrum [$N_e = (2-5) \times 10^5$]. The size distribution measured by EAS-TOP in single opera-

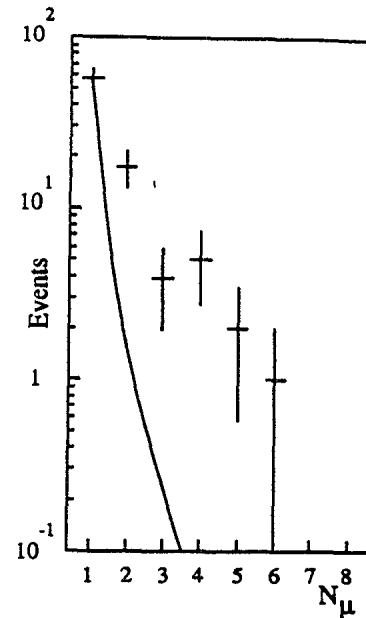


FIG. 8. Muon multiplicity distribution as observed in MACRO for the coincident internal events. The continuous curve is the muon multiplicity distribution as observed in MACRO alone, from any direction ($\theta \leq 70^\circ$) for a period of 1740 h of live time, normalized at $N_\mu = 1$.

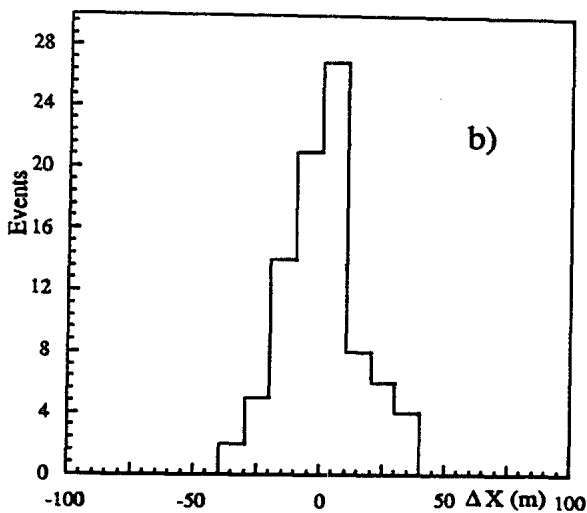
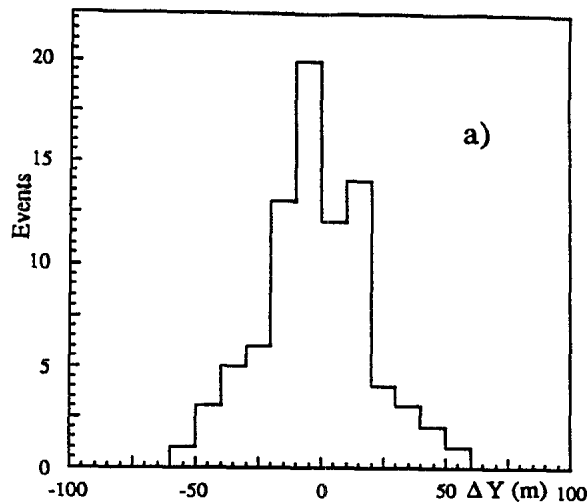


FIG. 7. Difference of the reconstructed core location, for the coincident internal trigger events ($\psi \leq 5^\circ$), projected on two orthogonal axes on a plane perpendicular to the direction EAS-TOP-MACRO.

tion is superimposed. Since in this case there is no request for high-energy muon production, the distribution is shifted toward lower shower size.

We have also tested the MACRO core location as an input to the EAS-TOP reconstruction code for the shower size. In Fig. 10 the reconstructed size is plotted versus the same quantity as obtained with the EAS-TOP data alone, when the multiple-muon events are selected in order to minimize the errors in the core location. The obtained result confirms the assumption of the accuracy in the backpointing of the underground muons. This can be of great importance in the analysis of the edge events.

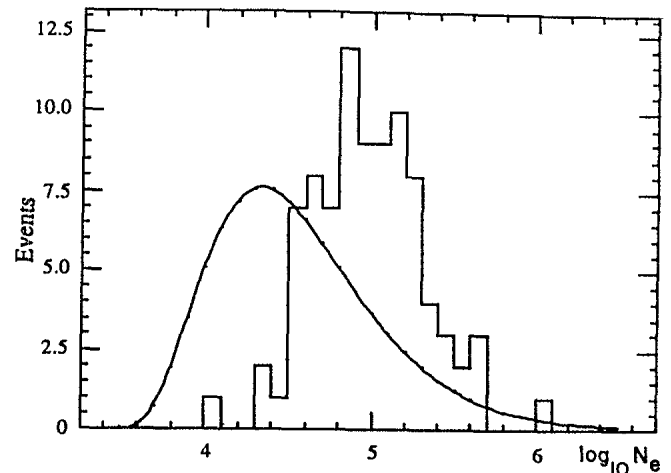


FIG. 9. Distribution of $\log_{10} N_e$ as measured by EAS-TOP for the coincident internal trigger events. The continuous line is the shape of the same distribution as measured by EAS-TOP in single operation, normalized at the same number of the events.

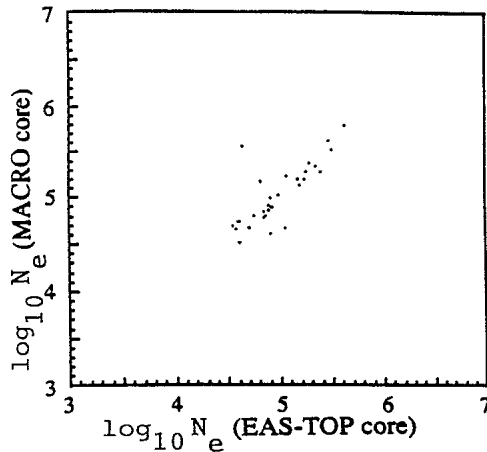


FIG. 10. Shower size reconstructed using the core location given by MACRO for multiple muon events vs the same quantity reconstructed by EAS-TOP alone.

We show in Fig. 11 the muon multiplicity distribution for the lower ($\log_{10} N_e < 4.8$) and higher ($\log_{10} N_e > 5.2$) intervals of EAS size. Within the obvious statistical limits the trend is similar to that shown previously in Fig. 8 and in Fig. 12 described in the next section: higher primary energy corresponds to longer high multiplicity tail.

VI. ANTICORRELATED EVENTS

Physical information can be obtained also from anticorrelated events. These are those events in which MACRO points to EAS-TOP but no coincidence is found, the shower energy being under threshold. These events come from the lower-energy region of the measurable spectrum, around $E_0 = 10^{13} - 10^{14}$ eV. Here the primary composition is better known than at higher ener-

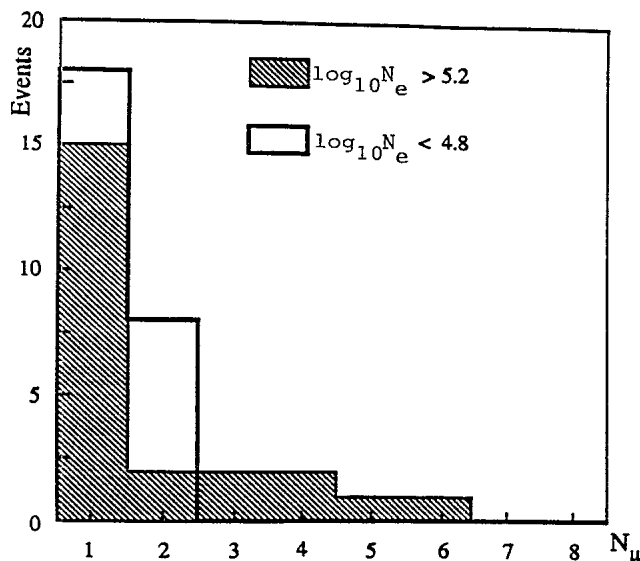


FIG. 11. Muon multiplicity distributions as observed by MACRO for coincidence events with $\log_{10} N_e > 5.2$ and $\log_{10} N_e < 4.8$.

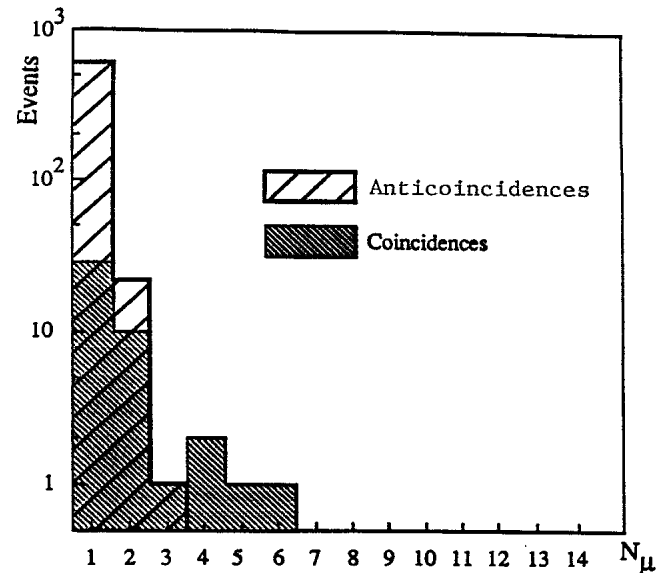


FIG. 12. Muon multiplicity distributions as observed by MACRO for events pointing to the fiducial region for coincident events, and anticoincident events.

gies. Furthermore, here the underground muons are mainly produced by the light nuclei (p and α). Therefore this measurement can provide an independent check of the analysis coming from the coincidence data.

A fiducial area of 10^4 m² has been chosen well inside the internal region of EAS-TOP, at least 50 m far from the edge of the array. In the total period of analysis, an anticoincidence/coincidence ratio of 624/44 has been found in the fiducial region. The statistical error ($\sim 20\%$) does not permit any definite conclusion now.

Figure 12 shows the muon multiplicity distributions as measured in the fiducial region for coincidence superimposed to the same distribution for anticoincidence events. The anticoincidences are mostly low-multiplicity events: the higher multiplicities (≥ 4) have been all detected as coincidence events, as one should expect, since they correspond to higher energies.

VII. CONCLUSIONS

The presented results demonstrate that the coincidence at the Gran Sasso Laboratory between EAS-TOP and MACRO has achieved good performance characteristics. In particular a good geometrical reconstruction of the events has been obtained, without systematic effects. This allows the simultaneous detection of underground muons and EAS, thus resulting in a powerful tool for the analysis of cosmic rays at very high energy. In this respect the two combined experiments have already shown their potential capability to perform accurate measurements in the most interesting region of the primary spectrum, ranging from the energies just below the knee up to about 10^4 TeV.

The presented results show the expected increase in

mean muon multiplicity as the measured energy increases in the extensive air shower array. Future improvements to both apparatus and the expected increase of statistics by about two orders of magnitude over the new few years should allow determinations of the composition of the primaries below and above the "knee" in the cosmic-ray flux spectrum.

ACKNOWLEDGMENTS

We gratefully acknowledge the technical support provided by the Gran Sasso National Laboratory and by our home institutions. This work was supported in part by the Department of Energy and the National Science Foundation.

¹For a general compilation of data, see A. M. Hillas, Phys. Rep. 20, 59 (1975), and for a recent compilation of data see J. Linsley, in *18th International Cosmic Ray Conference, Bangalore, India, 1983, Conference Papers*, edited by N. Durgaprasad *et al.* (Tata Institute of Fundamental Research, Bombay, 1983), Vol. 12, p. 135.

²A review of EAS experiments at energies above 10^{13} eV can be found in J. N. Stamenov, in *Proceedings of the Twentieth International Cosmic Ray Conference, Moscow, USSR, 1987*, edited by V. A. Kozyarivsky *et al.* (Nauka, Moscow, 1987), Vol. 8, p. 258.

³A review of data from underground muon experiments can be found in V. S. Narasimham, in *Proceedings of the Twentieth International Cosmic Ray Conference* (Ref. 2), p. 288.

⁴P. H. Barret *et al.*, Rev. Mod. Phys. 24, 133 (1952).

⁵E. Bellotti, Nucl. Instrum. Methods A264, 1 (1988).

⁶B. S. Acharya *et al.*, in *18th International Cosmic Ray Conference, Bangalore, India, 1983, Conference Papers* (Ref. 1), Vol. 9, p. 191.

⁷S. Corbato *et al.*, in *Proceedings of the Second International Symposium on Underground Physics, Baksan, 1987* (Institute of Nuclear Research of Academy of Science of USSR, Baksan, USSR, 1988), p. 171.

⁸M. Aglietta *et al.*, Nucl. Instrum. Methods A277, 23 (1989).

⁹K. Greisen, in *Progress in Cosmic Ray Physics* (North-Holland, Amsterdam, 1956), Vol. 3.

¹⁰M. Calicchio *et al.*, Nucl. Instrum. Methods A264, 18 (1988).

¹¹T. K. Gaisser and T. Stanev, Nucl. Instrum. Methods A235, 183 (1985).